Journal of Molecular Histology (2021) 53:51–62
https://doi.org/10.1007/s10735-021-10041-x

ORIGINAL PAPER

MicroRNA-126-5p inhibits apoptosis of endothelial cell in vascular arterial walls via NF-κB/PI3K/AKT/mTOR signaling pathway in atherosclerosis

Wei Jia[1] · Jianlong Liu[1] · Xuan Tian[1] · Peng Jiang[1] · Zhiyuan Cheng[1] · Cuijing Meng[2,3]

Received: 6 July 2021 / Accepted: 5 November 2021 / Published online: 4 January 2022

Abstract

Atherosclerosis is considered as a chronic inflammatory disease. MicroRNA-126-5p (miR-126-5p) may be pathophysiological relevant with the apoptotic processes in the endothelial cells in the arterial wall. Here, this study determined the role of circulating atherosclerosis-regulatory miR-126-5p in atherosclerotic mice and explored the possible mechanism in human aortic endothelial cells (HAECs). Atherosclerotic mice model was established, oxidative stress-induced apoptosis of HAECs was analyzed, and nuclear factor kappa B (NF-κB)/PI3K/AKT/mTOR signaling pathway was investigated both in vitro and in vivo. This study showed that miR-126-5p mice had less coronary atherosclerotic plaque and lower blood lipid than control mice after being induced by high cholesterol diet. Apoptosis of endothelial cells was inhibited and NF-κB/PI3K/AKT/mTOR signal pathway was downregulated in miR-126-5p mice compared to control. MiR-126-5p increased proliferation and inhibited apoptosis of HAECs induced by oxidative stress. In vitro assay showed that miR-126-5p regulated apoptosis of HAECs via downregulation of NF-κB-mediated PI3K/AKT/mTOR signaling pathway. In conclusion, these data indicated that transfection of miR-126-5p rescued apoptosis of HAECs and limited atherosclerosis, introducing a potential therapeutic approach for atherosclerosis.

Keywords Atherosclerosis · miR-126-5p · HAECs · Apoptosis · Oxidative stress · NF-κB · PI3K/AKT/mTOR

Introduction

Atherosclerosis is one kind of cardiovascular diseases and characterized by an accumulation of cholesterol deposits in macrophages in arteries (Homan et al. 2010; Lenato et al. 2007; Tabibiazar et al. 2005). The cholesterol deposition results in the formation of foam cells and dysfunction of endothelial cell within the arterial wall, which gradually shortens the cross section area of vessel lumen and impedes blood flow (Viiri et al. 2013; von zur Muhlen et al. 2012; Sookoian et al. 2011). The World Health Organization (WHO) predicts that global economic prosperity leads to the changes of dietary habit, which results in an epidemic of atherosclerosis in developing countries (Altin et al. 2016). As human vascular endothelial cells injury/inflammation and membrane disintegration are related to the initiation of atherosclerosis, and endothelial cells injury may explain the possible mechanism of inflammation-mediated atherosclerosis (Yamawaki and Iwai 2006). In addition, atherosclerosis-associated endothelial cell apoptosis results from downregulation of B-cell lymphoma-2 (Bcl-2) in high-fat diet (HFD)-induced atherosclerosis (Zhang et al. 2015a). Endothelial cells can release several types of membrane-bound extracellular vesicles including exosomes, microvesicles or microparticles, which may lead to increasing of apoptotic bodies during the formation of atherosclerosis (Paone et al. 2019). Furthermore, oxidative stress is involved in pro-atherogenic inflammatory cytokines, chemokines levels

✉ Wei Jia
weijiaprof@sina.com

✉ Cuijing Meng
cuijing_meng@163.com

[1] Department of Vascular Surgery, Beijing JiShuiTan Hospital, No 31, Xinjiekou East Road, Beijing 100035, People's Republic of China

[2] Department of 2nd Ophthalmology, The First Branch of Mudanjiang Medical University Affiliated Hongqi Hospital, Mudanjiang 157011, Heilongjiang, China

[3] The First Branch of Mudanjiang Medical University Affiliated Hongqi Hospital, No 5 Township Road, Mudanjiang 157000, Heilongjiang, China

and endothelial injury, which may constitute a pathway for accelerated atherosclerosis in atherosclerosis patients (Dussault et al. 2014).

Atherosclerosis is a disease caused by lipid-induced inflammation of the vessel wall orchestrated by a complex interplay of various cell types including macrophages, smooth muscle cells, and endothelial cells (Rotllan et al. 2013). MicroRNAs are short non-coding RNAs, which are involved in sequence-specific post-transcriptional regulation of gene expression during the pathological process atherosclerosis (Bouchareychas and Raffai 2018). MicroRNAs play a critical role in modulating vascular smooth muscle cells and endothelial cells, which may be one of initial cellular events in the development of atherosclerosis and represent new therapeutic target for atherosclerosis (Chen et al. 2012; Xu et al. 2012; Zhang 2009). Jiang et al.have found that miR-126-5p can decrease endothelial repair and lesion size via inhibiting apoptosis and formation of atherosclerotic lesion (Boon and Dimmeler 2014). The effect of miR-126-5p on atherosclerosis has been identified in vivo, which controls differentiation of smooth muscle cells, promotes lesion formation, whereas the endothelial cell-specific miR-126-5p signals the need for endothelial repair through its transfer from apoptotic endothelial cells in microvesicles (Wei et al. 2013). Additionally, miR-126-5p inhibits apoptosis of endothelial cells by directly targeting transient receptor potential channel 6 (TRPC6) (Zhang et al. 2015b). However, the mechanism underlying the role of miR-126-5p in oxidative stress-induced apoptosis of endothelial cell remains to be further addressed.

In the present study, we investigated the role of miR-126-5p in HFD-fed apolipoprotein E-deficient ($apoE^{-/-}$) mice and oxidized low-density lipoprotein (ox-LDL)-treated HAECs. This study also analyzed the atherosclerotic lesions and blood lipid level in $apoE^{-/-}$ mice fed with HFD. Here, we reported that miR-126-5p overexpression decreased coronary atherosclerotic plaque and blood lipid, as well as decreased apoptosis of HAECs via downregulation of nuclear factor kappa B (NF-κB)-mediated PI3K/AKT/mTOR signaling pathway. Therefore, miR-126-5p may serve as a potential therapeutic molecular for atherosclerosis therapy.

Materials and methods

Animal models and quantification of atherosclerotic lesions

A total of 40 male $apoE^{-/-}$ mice (6 weeks old; weight, 23 ± 6 g) and wild-type C57BL/6 J controls (6 weeks old; weight, 22 ± 8 g, n = 20) were obtained from the Charles River Laboratory Animal Co, Ltd (Beijing, China). All mice were housed under a 12 h light and dark cycle, 23 ± 2 °C, 55% ± 5% humidity with free access to food and water. All mice were fed with HFD (10% cholesterol, 10% lard, 2% cholate, and 78% basal feed) for 12 weeks to induce atherosclerosis. The generation of miR-126-5p transgenic mice was performed as described previously (Lyu et al. 2018). Expression level of miR-126-5p was examined in each mouse. All $apoE^{-/-}$ mice were randomly divided into two groups (n = 20/group): miR-control group (miR-NC), and hsa-miR-126-5p (miR-126-5p) group. Wild-type C57BL/6 J mice were used as healthy control (n = 20). The $apoE^{-/-}$ mice were received intravenous injection with miR-NC (40 mg/kg) or miR-126-5p (30 mg/kg) one time a day by tail vein for 30 consecutive days after starting HFD. Mice were sacrificed after anesthesia using pentobarbital sodium (50 mg/kg IP). The mice were sacrificed on day 31 by using cervical decapitation and the aortic sinuses were collected and stored in liquid nitrogen for further analysis. The animal experiments were approved by the Beijing JiShuiTan Hospital and conducted in accordance with the National Institutes of Health Guidelines on the Use of Laboratory Animals.

Histological evaluation of atherosclerotic lesions

Aortic sinuses were fixed with 4% paraformaldehyde, dehydrated, embedded in paraffin, and sectioned into 4-μm sections. Tissue sections were stained with hematoxylin and eosin (H&E, Sigma-Aldrich) for 5 min at 25 °C, washed with PBS and then imaged using a light microscope (Olympus Corp., Tokyo, Japan) For atherosclerotic lesion examination in aortic sinuses. Aortic sinus tissue sections were immersed in 100% isopropanol (Sigma-Aldrich) for 12 h at 25 °C and stained with Evans blue (Sigma-Aldrich) for 30 min at 25 °C to examine atherosclerotic plaque formation in atherosclerotic lesions. In addition, tissues sections were incubated 60% isopropanol for 5 min and then stained with oil red O (Bio-technology, USA) solution for 15 min and rinsed in PBS followed by counterstained with hematoxylin for 20 min at 25 °C. Atherosclerotic lesion area in aortic sinus tissue was measured using Image Pro Plus Version 6.0 (Media Cybernetics, Inc., Rockville, MD, USA).

Immunohistochemistry

Antigen retrieval was performed using citrate buffer (PH.6.0) for 7 min at 100 °C followed by blocking with normal goat serum (CST, 5425S) for 1 h. Tissue sections were incubated rabbit anti-mouse primary antibody: α-SMA (1:1000; ab5694, Abcam), CD68 (1:1000; MCA1957, Bio-Rad AbD Serotec), rabbit MCP1 (monocyte chemoattractant protein 1; 1:1000; ab7202, Abcam), IL-6 (interleukin 6; 1:1000; MCA1490, Bio-Rad AbD Serotec), TNF-α (1:1000; ab6671, Abcam), type I (1:1000, ab34710, Abcam) and

type III collagen (1:1000, ab7778, Abcam) overnight at 4 °C. The sections were incubated with a goat anti-rabbit peroxidase-labeled anti-body (1:500, ab205719, Abcam) for 2 h at 25 °C. Tissue sections were visualized by applying ImmPACT DAB peroxidase substrate kit (Vector Laboratories, SK-4105). All slides were imaged under light microscope at ×400 magnification and results were quantified using a computer-assisted morphometric analysis system (Image-Pro Plus 5.0, Media Cybernetics, USA).

Plaque vulnerability index

Immunohistochemical staining was used to characterize plaque vulnerability by evaluating lipid-rich necrotic core size, thickness of the fibrous cap, plaque collagen and SMC contents, and macrophage contents as described previously (Wang et al. 2018). Briefly, plaque morphological histomorphometry characters were evaluated by hematoxylin and eosin and alizarin red S, trichrome staining, immunofluorescence staining for α-SMA (α-smooth muscle actin) and CD68. Plaque vulnerability index was calculated following the formula: (plaque vulnerability index) = (SMC area + collagen area)/(macrophage area + lipid area) × 100% (She et al. 2009).

Plaque rupture

Plaque rupture was analyzed using buried fibrous caps, a surrogate marker of plaque rupture by Elastica van Gieson (EVG) staining as described previously (Hermann et al. 2016). In brief, aortic sections (4 μm thick) were prepared and stained with Evans's blue (Sigma-Aldrich) for 30 min at 25 °C. After washing with PBS three times, tissue sections were stained with EVG (Sigma-Aldrich) for 15 min at 25 °C. Analysis was performed with a microscope with a computerized, digital image analysis system and ImageJ Software Version 2.0.

Blood lipids analysis

Blood samples (0.5 ml) from caudal vein were obtained from experimental mice on day 31. Serum was collected and obtained using centrifugation at 12,000 × g for 10 min at 4 °C. Total cholesterol (TC), triglyceride (TG), high-density lipoprotein cholesterol (HDL-C), and low-density lipoprotein cholesterol (LDL-C) levels were detected by a Hitachi 7600 Automatic Biochemical Analyzer (Hitachi High-Technologies, Japan).

Cell culture

Human aortic endothelial cells (HAECs) were purchased from the American Type Culture Collection (Manassas, VA, USA, https://www.atcc.org/). Cells were cultured in endothelial growth medium-2 (EGM-2) supplemented with growth factors, 10% fetal bovine serum (FBS; Thermo Fisher Scientific), 100 U/ml penicillin/streptomycin at 37 °C in a 5% CO_2 incubator. To induce oxidative stress in vitro, HAECs were treated with 100 μg/ml of ox-LDL (Invitrogen) for 24 h at 37 °C in a 5% CO_2 incubator for further analysis (Kattoor et al. 2017).

TUNEL assay

To quantify the apoptosis of HAECs, the level of DNA fragmentation was detected using an In Situ Cell Death Detection Kit (Roche Applied Science, Indianapolis, IN, USA) according to the manufacturer's instructions. HAECs were mounted in SlowFade containing DAPI (Sigma-Aldrich) and observed under the fluorescence microscope. Apoptotic cells were quantified as follow: The apoptotic index = (number of apoptotic cells)/(total number of cells).

MicroRNA and NF-κB transfection

MiR-126-5p (5′-UCGUACCGUGAGUAAUAAUGCG-3′) and a negative control (MiR-NC, 5′-UUCUCCGAA CGUGUCACGUTT′) were purchased from GenePharma (Shanghai, China). HAECs were cultured in 6-well plate when grown to 70–80% confluence. MiR-126-5p (100 nM) and miR-NC (100 nM) were transfected into HUVECs using Lipofectamine 2000 (Invitrogen, Carlsbad, CA) following the manufacturer's instructions. After 72 h, the transfected HUVECs were treated with 100 μg/ml of ox-LDL in serum-free medium for 12 h to further analysis. Vectors of pcDNA-NF-κB (pNF-κB), and pcDNA empty vector (pControl) were obtained from GenePharma (Shanghai, China). HAECs or miR-126-5p-transfected HAECs were transiently transfected with pcDNA-NF-κB (2 μg) or pcDNA empty vector (2 μg) using Lipofectamine 2000 reagent (Invitrogen, Carlsbad, CA, USA). After 72 h transfection, HAECs were exposed to 100 μg/ml of ox-LDL in serum-free medium for 12 h to further analysis.

Quantitative real-time PCR (QRT-PCR)

Total RNA was extracted from HUVECs or aortic sinuses using RNeasy Mini kit (Invitrogen Life Technologies, Carlsbad, USA). 1 μg of RNA was reverse transcribed into cDNA using cDNA Synthesis Kit (Roche, Shanghai, China) according to the manufacturer's instructions. The primer sequences were listed in Table 1. QRT-PCR was performed using PrimeScript RT reagent Kit (TAKARA, Otsu, Japan) following the manufacturer's protocol. Expression of miR-126-5p was analyzed using mirVana™ qRT-PCR miRNA measurement kit (Ambion, Austin, USA) according to the manufacture's

Table 1 Sequences of primers

	Forward	Reverse
MiR-126-5p	5′-GTGGTGGTGGTGTGTGTGTGTTT-3′	5′-CTCAACCCAACCCAAACAACAACCA-3
U6	5′-CTCGCTTCGGCAGCACA-3′	5′-AACGCTTCACGAATTTGCGT-3′
NF-κB	5′-CATGCTGATGGAGTACCCTGAAGC-3′	5′-CATGTCCGCAATGGAGGAGAAG-3′
β-actin	5′-GTACCACCATGTACCCAGGC-3′	5′-AACGCAGCTCAGTAACAGTCC-3′

instrument. The mRNA level of NF-κB was performed using a SYBR-Green qRT-PCR assay (Takara Bio, Inc.) incorporation method on ABI 7500 fast Real-Time PCR system (Applied Biosystems), with β-actin as an internal control. The relative mRNA level was determined as values of $2^{-\Delta\Delta Ct}$. The relative expression level of miR-126-5p was determined using TaqMan MicroRNA Assay Kit (Applied Biosystems), with U6 as an internal control.

Western blot analysis

Proteins in the treated HUVECs (5×10^6) were extracted using RIPA buffer (Sigma-Aldrich). A Bicinchoninic acid assay (BCA, Thermo Fisher Scientific, USA) assay was used to determine concentrations of protein. Proteins (40 µg) were separated using Sodium dodecyl sulfate polyacrylamide gel electrophoresis (SDS-PAGE), transferred to polyvinylidene fluoride membrane (Bio-Rad, CA, USA) and then blocked with 5% BSA (Sigma-Aldrich) overnight at 4 °C. Membrane was washed with Tris–HCl buffer solution-Tween (TBST) and incubated with the primary antibodies: nuclear NF-κB (ab19285), PI3K (ab32089), Akt (ab8805), mTOR, (ab2732), phosphorylated NF-κB (pNF-κB, ab194908) phosphorylated PI3K (pPI3K, ab182651), phosphorylated AKT (pAKT, ab8933) phosphorylated mTOR (pmTOR, ab109268), caspase-3 (ab13847), PARP (ab32064), cytochrome C (ab133504), PPAR (ab45036), and β-actin (ab8226, all 1:1000 dilutions, All purchase from Abcam, USA) overnight at 4 °C followed by incubation with the horseradish peroxidase (HRP)-conjugated secondary antibody overnight at 4 °C. The protein bands were examined using electrochemiluminescence (ECL, Pierce, Rockford, USA) method and band intensities were analyzed using a BioSpectrum Gel Imaging System v4.6 (Bio-Rad, Hercules, CA).

Cell proliferation assay

Cell proliferation was detected using cell counting Kit-8 (CCK-8, Thermo Fisher Scientific, USA) assay according to the manufacture's instrument. Briefly, the treated HUVECs (1×10^3) were cultured in a 96-well plate for 24 h at 37 °C. Cells were then incubated with 10 µl of CCK-8 solution for 30 min at 7 °C. The absorbance at 450 nm was measured with a spectrophotometer (Thermo Electron Corporation, Vantaa, Finland).

Luciferase reporter assay

The 3′UTR sequences of NF-κB containing the putative binding sites of wild type (WT) or mutant (MUT) miR-126-5p were synthesized and inserted into pMIR-REPORT luciferase reporter plasmids (Promega, Madison, WI, USA) to construct NF-κB-WT-miR-126-5p or NF-κB-MUT-miR-126-5p, respectively. HAECs (1×10^5) were cotransfected with NF-κB-WT-miR-126-5p (50 nM), NF-κB-MUT-miR-126-5p (50 nM), or miR-NC using Lipofectamine 2000 reagent (Invitrogen, Carlsbad, CA, USA) according to the manufacturer's protocol. The relative luciferase activity was evaluated using a Dual-Luciferase Reporter Assay System (Promega) after 48-h transfection.

Statistical analysis

Data are expressed as mean ± standard deviation (SD) from three independent experiments. All statistical analyses were performed using SPSS version 18.0 software (SPSS Inc., Chicago, IL, USA). Two group comparisons were determined by Student's *t*-test and multiple groups was performed by one-way ANOVA analysis, followed by Dunnett's post hoc test. $p < 0.05$ was considered statistically significant.

Results

MiR-126-5p overexpression inhibits atherosclerotic lesions in HFD-induced apoE$^{-/-}$ mice

To verify the role of miR-126-5p in atherosclerosis, expression of miR-126-5p was investigated in the aorta tissue in apoE$^{-/-}$ mice. The results in Fig. 1A demonstrated that expression of miR-126-5p was significantly downregulated in the aorta tissue in apoE$^{-/-}$ mice compared to healthy mice. As depicted in Fig. 1B, injection with miR-126-5p upregulated miR-126-5p expression in the aorta tissue in apoE$^{-/-}$ mice compared to control. Pathological analyses demonstrated that miR-126-5p overexpression decreased area of coronary atherosclerotic plaque in aortic sinuses

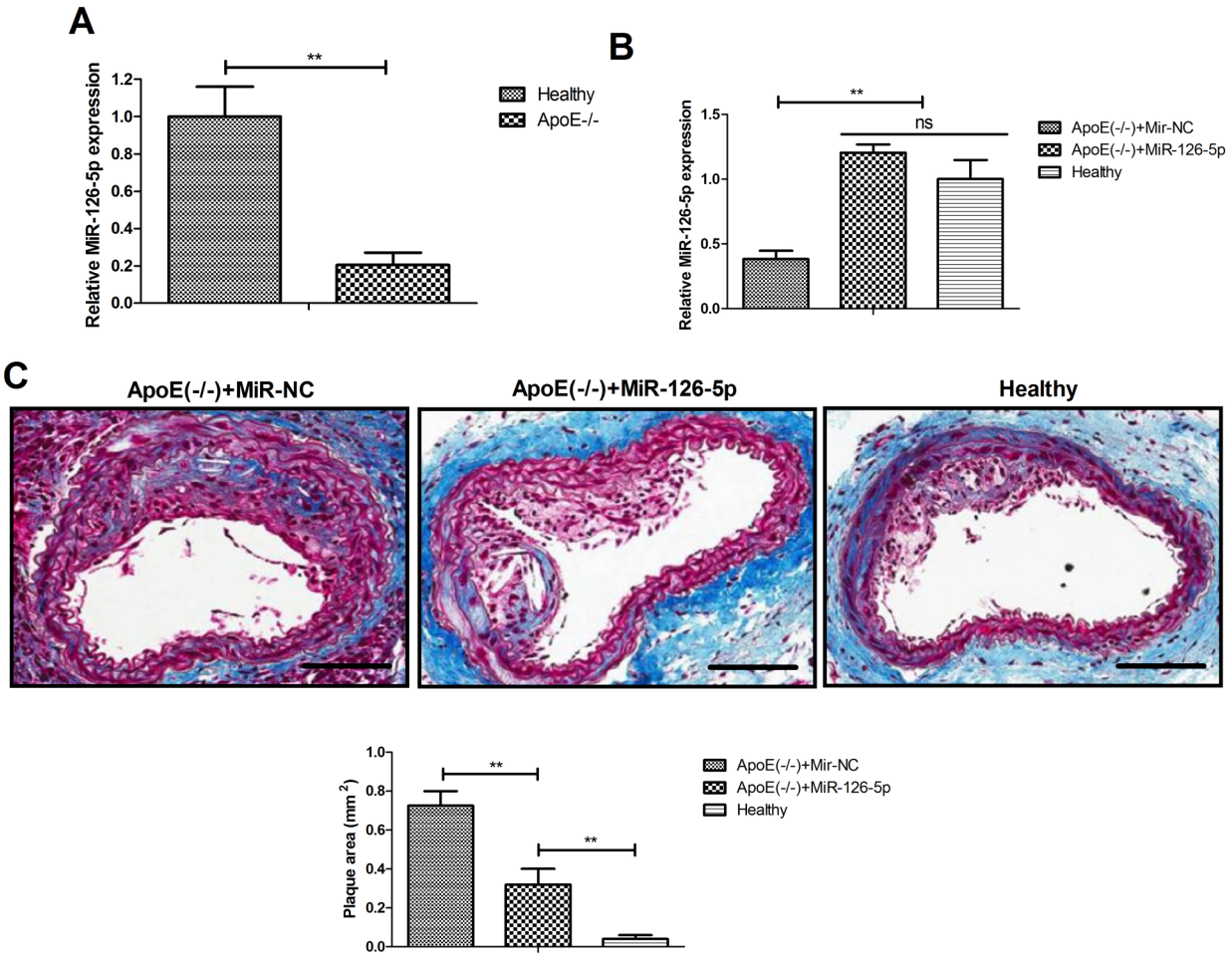

Fig. 1 Effects of miR-126-5p overexpression on atherosclerotic plaque extension in HFD-induced apoE$^{-/-}$ mice. **A** Expression of miR-126-5p in the aorta tissue between apoE$^{-/-}$ mice and healthy mice. **B** Effects of miR-126-5p on miR-126-5p expression in the aorta tissue in apoE$^{-/-}$ mice. **C** Formation of atherosclerotic plaque in experimental mice. **D** Staining of type I and type III collagen in the aorta tissue in experimental mice. **E** Effects of miR-126-5p on abdominal aortic segments determined by Oil red O staining. **F** The vulnerability index in miR-126-5p, miR-NC and healthy group. **p < 0.01 vs. miR-NC group

compared to control (Fig. 1C). Data showed that miR-126-5p decreased expression level of type I and type III collagen in apoE$^{-/-}$ mice compared to control (Fig. 1D). Oil red O in the abdominal aortic segments decreased in miR-126-5p group compared to control (Fig. 1E). The vulnerability index in miR-126-5p group was significantly higher than that in control (Fig. 1F).

MiR-126-5p overexpression decreases blood lipid profile in FD-induced apoE$^{-/-}$ mice

The effects of miR-126-5p injection on blood lipid metabolism were investigated in FD-induced apoE$^{-/-}$ mice. The blood lipid profile was statistically significant between miR-126-5p and control group (Table 2). Serum levels of TC, TG, HDL and LDL were downregulated by miR-126-5p in FD-induced apoE$^{-/-}$ mice compared to control. As shown in Fig. 2, miR-126-5p injection decreased the incidence of plaque rupture compared to control group, which was defined as fibrous cap disruption with luminal thrombosis.

MiR-126-5p overexpression promotes proliferation and inhibits apoptosis in ox-LDL-treated HAECs

The effects of miR-126-5p on proliferation and apoptosis of HAECs were further analyzed in vitro. As illustrated in Fig. 3A, expression of miR-126-5p was downregulated in ox-LDL-treated HAECs. Transfection of miR-126-5p increased the proliferation of HAECs following ox-LDL challenge (Fig. 3B). Meanwhile, TUNEL assay showed that miR-126-5p overexpression significantly inhibited apoptosis of ox-LDL-treated HAECs compared to miR-NC group (Fig. 3C). It demonstrated that miR-126-5p overexpression decreased apoptosis-related protein expression of PARP,

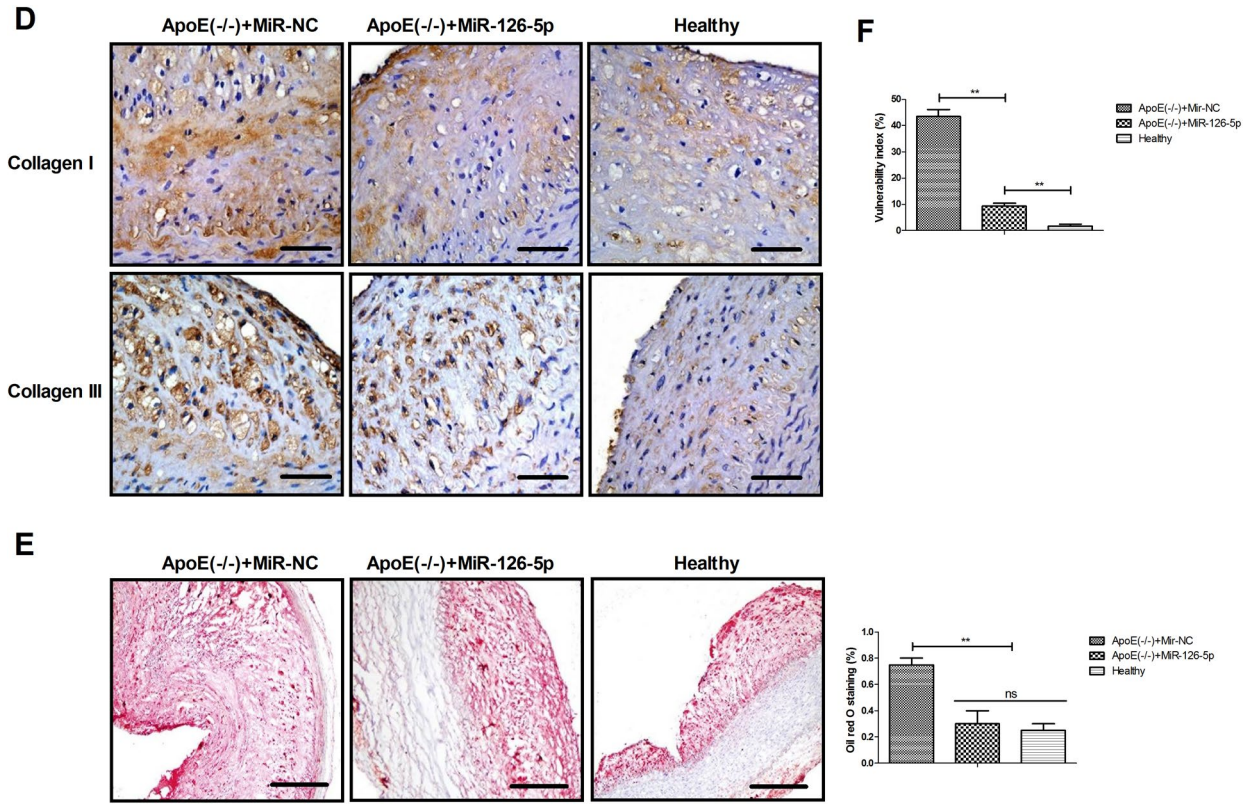

Fig. 1 (continued)

Table 2 Serum lipid profiles in experimental mice

	MiR-NC	MiR-126-5p	Healthy
TC (mmol/l)	31.44 ± 5.68	26.60 ± 8.42*	22.52 ± 8.36*#
TG (mmol/l)	3.42 ± 0.84	2.74 ± 0.96*	2.56 ± 0.88*
HDL (mmol/l)	2.25 ± 0.68	1.72 ± 0.90*	1.70 ± 1.02*
LDL (mmol/l)	27.74 ± 8.50	23.58 ± 6.75*	21.46 ± 7.40*#
VLDL (mmol/l)	25.22 ± 7.05	21.20 ± 3.62*	18.34 ± 4.11*#

TC total cholesterol, *TG* triglyceride, *HDL* high density lipoprotein, *LDL* low density lipoprotein, *VLDL* very low-density lipoprotein

*$P < 0.01$ vs. MiR-NC

#$P < 0.05$ vs. MiR-126-5p

Cleaved caspase-3 (C-caspase-3) and cytochrome C (Cyto c) in ox-LDL-treated HAECs (Fig. 3D).

NF-κB is a direct target of miR-126-5p in HAECs

The possible target of miR-126-5p was explored in ox-LDL-treated HAECs. As described previously, NF-κB was reported to play a crucial role in the development of atherosclerosis, which was identified as a potential target of miR-126-5p. To verify our hypothesis, the MUT 3'-UTR or WT sequences of NF-κB containing the putative binding sites of miR-126-5p were inserted into pMIR-REPORT plasmids. Luciferase reporter assay demonstrated that miR-126-5p overexpression decreased luciferase activity of the 3′UTR of NF-κB in ox-LDL-treated HAECs (Fig. 4A). Data showed that miR-126-5p overexpression inhibited NF-κB and phosphorylated NF-κB (pNF-κB) expression in ox-LDL-induced HAECs compared to miR-NC. Overexpression of miR-126-5p also decreased pNF-κB/NF-κB in ox-LDL-induced HAECs (Fig. 4B).

MiR-126-5p overexpression suppresses the NF-κB-mediated PI3K/AKT/mTOR pathway in ox-LDL-treated HAECs

To identify the potential mechanism of miR-126-5p in ox-LDL-treated HAECs, PI3K/AKT/mTOR signaling pathway was analyzed in HAECs. QRT-PCR showed that pCDNA-NF-κB transfection increased NF-κB mRNA expression in ox-LDL-treated HAECs (Fig. 5A). Western blot analyses revealed that miR-126-5p overexpression suppressed the protein level of phosphorylated PI3K, AKT and mTOR in ox-LDL-treated HAECs, while NF-κB overexpression recuperated and abolished miR-126-5p (NF-κB/

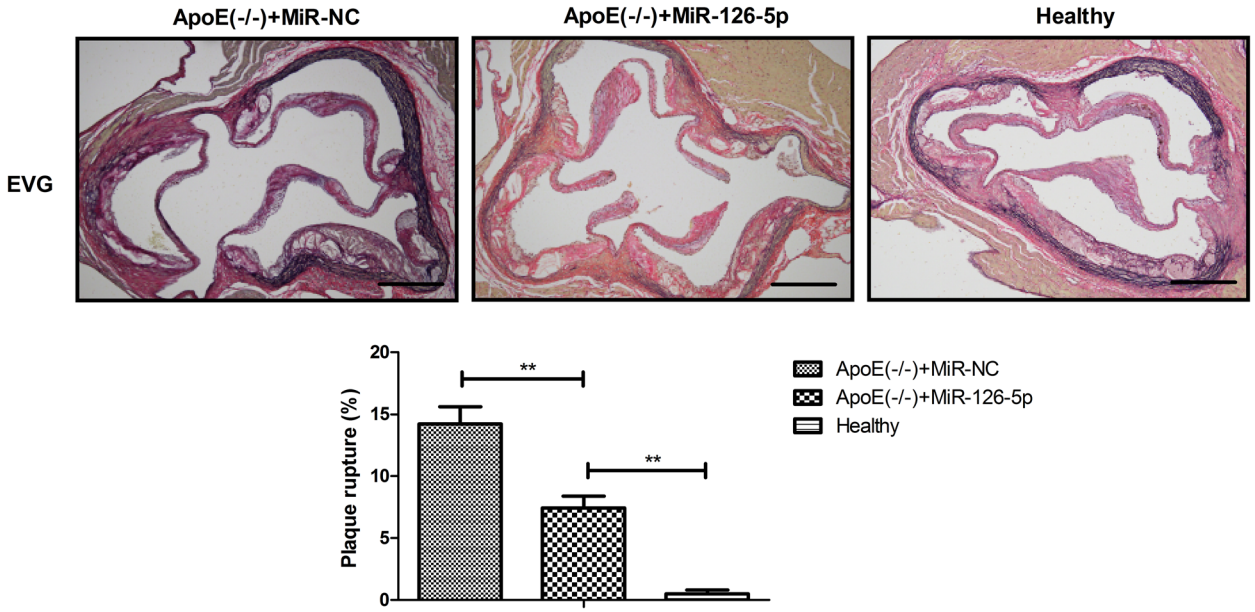

Fig. 2 Effects of miR-126-5p overexpression on plaque rupture in FD-induced apoE$^{-/-}$ mice. MiR-126-5p injection decreased the incidence of plaque rupture compared to control group. **p < 0.01 vs. miR-NC group

miR-126)-regulated PI3K/AKT/mTOR in ox-LDL-treated HAECs (Fig. 5B).

NF-κB overexpression antagonizes the miR-126-5p-regulated proliferation and apoptosis in ox-LDL-treated HAECs

The effects of NF-κB overexpression on miR-126-5p-regulated proliferation and apoptosis were investigated in ox-LDL-treated HAECs. As shown in Fig. 6A, NF-κB overexpression antagonized the miR-126-5p-increased proliferation of HAECs induced by ox-LDL (Fig. 6A). Data demonstrated that miR-126-5p-inhibited apoptosis of HAECs induced by ox-LDL was canceled by NF-κB overexpression (Fig. 6B).

Discussion

The discovery of the potential role of microRNAs in atherosclerosis sheds light on the pathological processes of atherogenesis and may provide novel therapies options for cardiovascular diseases (Santovito et al. 2012; Schober et al. 2012; Busch and Zernecke 2012). In particular, miR-126-5p decreases atherosclerotic lesion formation in apoE$^{-/-}$ atherosclerotic mice model (Boon and Dimmeler 2014). Thus, analysis of target gene of putative miR-126-5p targets plays a vital role to find the treatment options for atherosclerotic disease. In the present study, apoE$^{-/-}$ atherosclerotic mice model and ox-LDL-treated HAECs cell model were established to investigate the possible mechanism of miR-126-5p. Here, findings showed that miR-126-5p presented protective effects against atherosclerosis via decreasing apoptosis and coronary atherosclerotic plaque in aortic sinuses in apoE$^{-/-}$ atherosclerotic mice. Our data demonstrated that miR-126-5p decreased oxidative stress-induced apoptosis of endothelial cell in vascular arterial walls via PI3K/AKT/mTOR signaling pathway in atherosclerosis rat model.

Apoptosis of endothelial cell plays a crucial role in biochemical characteristics and potential implications for atherosclerosis, which may enable a greater understanding of disease pathogenesis and foster the development of new therapies (Choy et al. 2001). Analysis of these data identified that miR-126-5p significantly decreased apoptosis of endothelial cell in vascular arterial walls and inhibited the formation of coronary atherosclerotic plaque in aortic sinuses in apoE$^{-/-}$ atherosclerotic mice. Functional blockade of PARP reduces atherosclerotic lesion development by moderating invasion and activation of dendritic cells and T cells (Erbel et al. 2011). Caspase-3 is independently associated with coronary calcium, abdominal aortic wall thickness, and aortic compliance, suggesting a link between apoptosis and atherosclerosis (Matulevicius et al. 2008). It found that miR-126-5p downregulated PARP and Caspase-3 in ox-LDL-treated HAECs compared to control. A previous study has found that oxidative stress is a link between endothelial injury and atherosclerosis in haemodialysis patients, which may constitute a pathway for accelerating atherosclerosis in haemodialysis patients (Pawlak et al. 2004). Reduction of oxidative stress and inflammation in the injured arteries is

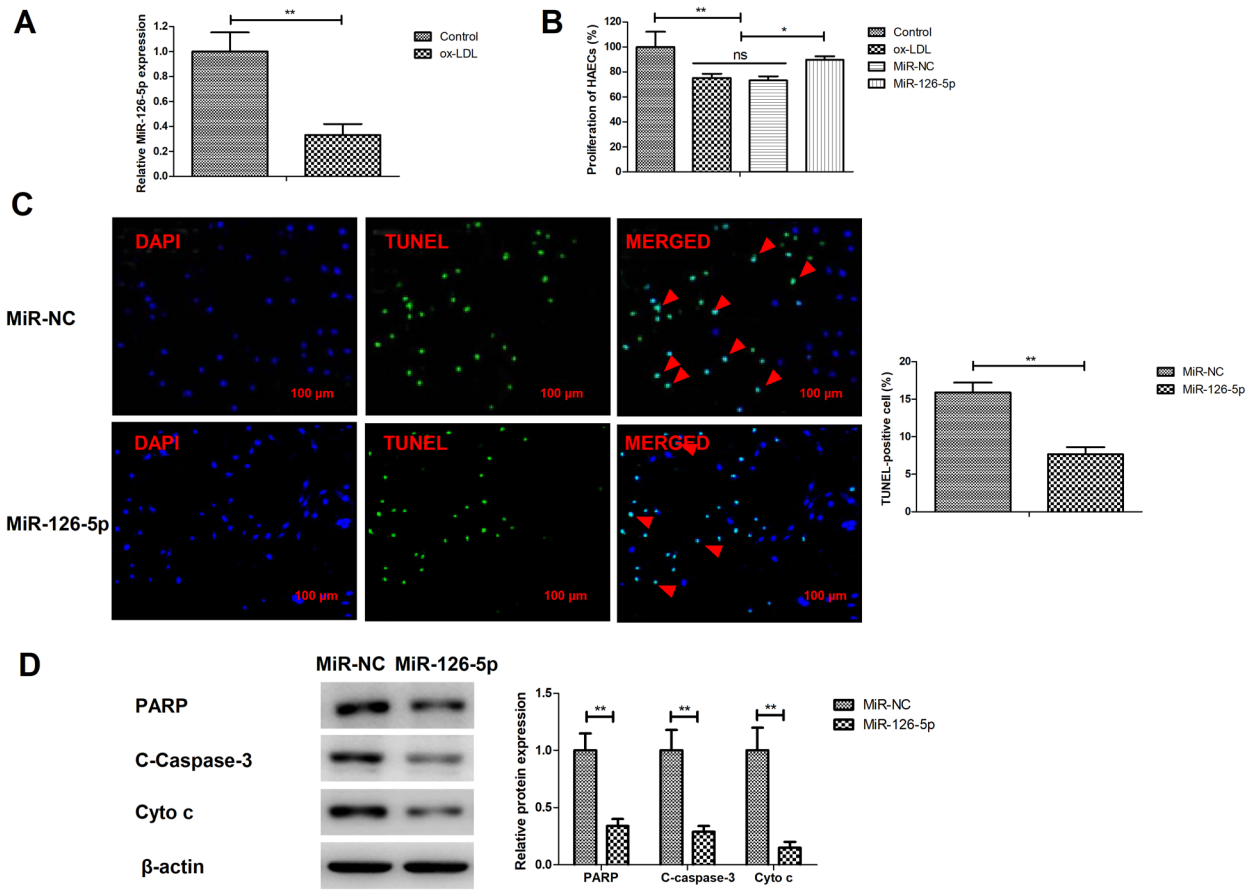

Fig. 3 Effects of miR-126-5p overexpression on proliferation and apoptosis in ox-LDL-treated HAECs. **A** Expression of miR-126-5p in ox-LDL-treated HAECs after transfection with miR-126-5p. **B** Proliferation of ox-LDL-treated HAECs after transfection with miR-126-5p or miR-NC. **C** Apoptosis of ox-LDL-treated HAECs after transfection with miR-126-5p or miR-NC. **D** Protein expression of PARP, Cleaved caspase-3 and Cytochrome C in ox-LDL-treated HAECs after transfection with miR-126-5p or miR-NC. **p < 0.01 vs. miR-NC group

involved in lowering of blood cholesterol levels in patients with atherosclerosis (Dussault et al. 2014). In this study, results found that antioxidant effect mediated miR-126-5p decreased oxidative stress-induced apoptosis of endothelial cell in vascular arterial walls.

A study has shown that mature dendritic cell increases endothelial inflammation and atherosclerosis via TNF-α mediated NF-κB pathway, which provides a potential method to prevent endothelial inflammation and atherosclerosis (Gao et al. 2016). Inhibition of NF-κB signaling has been shown to protect against atherosclerosis by regulation of lipid metabolism (Yu et al. 2015). This study aimed to discuss the associations between miR-126-5p and NF-κB in lipid metabolism in atherosclerotic mice and to implicate the potential therapeutic benefits of miR-126-5p. Data demonstrated that miR-126-5p regulated proliferation and apoptosis in ox-LDL-treated HAECs by targeting NF-κB signal pathway. Tang et al.have found that miR-126-5p alleviates endothelial cells injury in atherosclerosis by inhibition of PI3K/Akt/mTOR pathway (Tang and Yang 2018). However, activating PI3K/Akt/mTOR signaling pathway promotes cell proliferation, survival, and migration of vascular smooth muscle cells and endothelial cells, which are two key factors in the formation of atherosclerosis (Yao et al. 2018). A study has indicated that activating the PI3K/Akt pathway and inhibiting activation of NF-κB inhibits tissue factor expression in HUVECs (Deng et al. 2017). Another study has showed that PI3K/Akt/eNOS and NF-κB pathways are involved in Methylglyoxal-induced oxidative stress and apoptosis (Chu et al. 2017). Reversely, data in this study found that NF-κB expression was inhibited by miR-126-5p, which further led to decreasing of PI3K/Akt/mTOR expression in HAECs. Data also demonstrated that miR-126-5p decreased PI3K/Akt/mTOR pathway via targeting NF-κB signal pathway in HAECs. These data indicated that NF-κB might be an upstream molecular of PI3K/Akt/mTOR that served as a promising therapeutic target for patients with atherosclerosis. However, the effect of miR-126-5p on

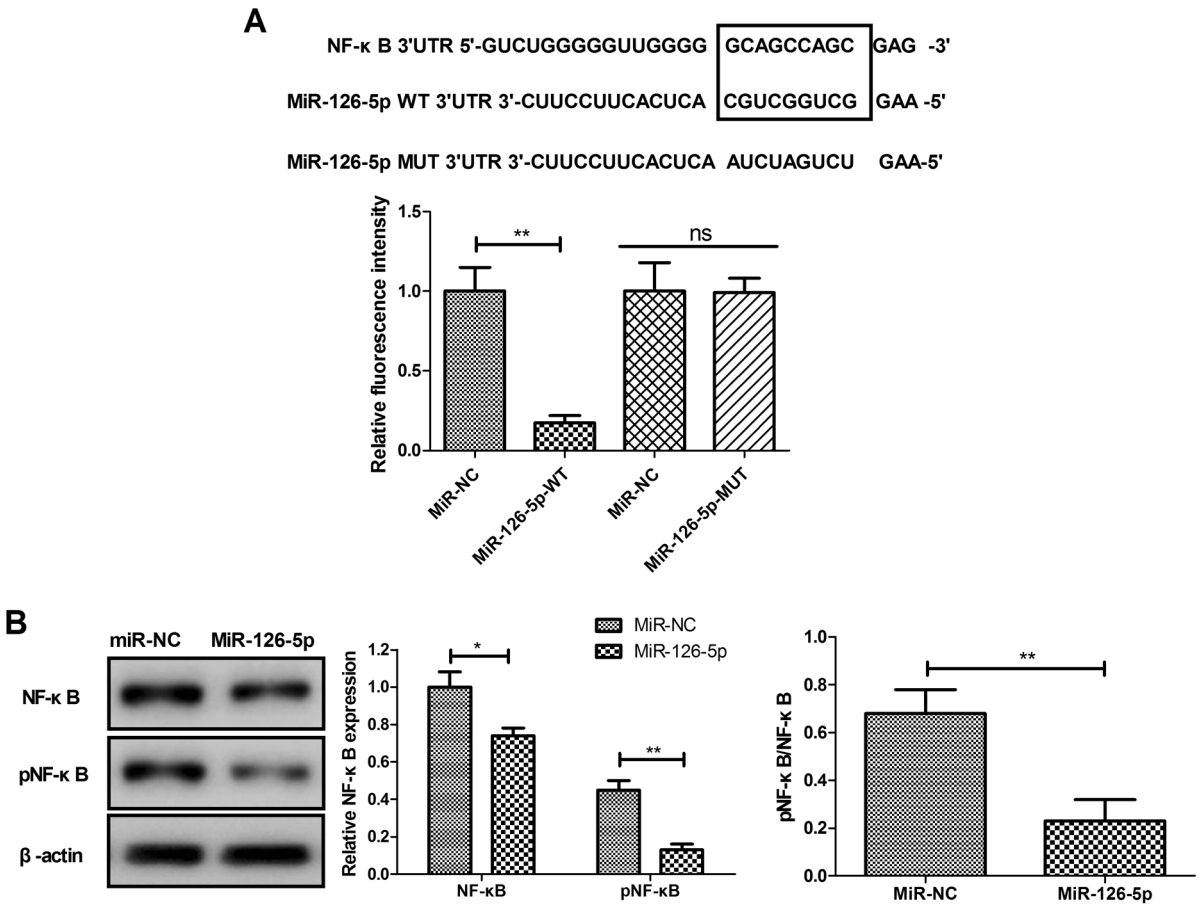

Fig. 4 NF-κB is a direct target of miR-126-5p in HAECs. **A** NF-κB was identified as the candidate target gene of miR-126-5p determined by miR-126-5p. **B** Effects of miR-126-5p on NF-κB and phosphorylated NF-κB (pNF-κB) expression in ox-LDL-treated HAECs. $^{**}p < 0.01$ vs. miR-NC group

decreasing of pNF-κB/NF-κB in HAECs and other mechanisms of endothelial cell injury should perform in our future work.

A study has shown that miR-126-5p regulates apoptosis of granulosa cells via Wnt and Akt signal pathway (Mao et al. 2018). In addition, Chen et al. has found that the apoptosis of vascular endothelial cells is increased by miR-126 inhibition and PI3K/Akt signal transduction is suppressed by miR-126-5p inhibition (Chen et al. 2016). The transfection with miR-126 inhibitor into endothelial cells suppresses Ox-LDL-induced cell apoptosis, thereby persistently activating the PI3K/Akt signaling pathway (Li et al. 2019). Consistent with these findings, we found that miR-126-5p overexpression suppressed the NF-κB-mediated PI3K/AKT/mTOR pathway in ox-LDL-treated HAECs. Notably, our data found that miR-126-5p did not affect total protein levels, but reduce phosphorylated protein levels, suggesting an absence of miR-126-5p by other factors.

These are several novelties in this study. First, the regulatory mechanism of miR-126-5p was identified in crosstalk between NF-κB and PI3K/AKT/mTOR pathway in the atherosclerotic pathology. Second, data in this study demonstrated that miR-126-5p is involved in apoptotic networks and played a vital role in the atherosclerotic progression. Third, miR-126-5p might represent a novel therapeutic application, which contributed to clarify the metastatic mechanism of atherosclerosis.

Some limitations of this study should be noted. First, this study did not investigate the role of miR-126-5p in clinical patients with atherosclerosis. Second, miR-126-5p expression in artery atherosclerotic plaque did not analyze in vivo. Third, the effect of miR-126-5p on other signal pathways did not investigate in ox-LDL-treated HAECs. Therefore, further study should investigate the role of miR-126-5p in the atherosclerotic pathology in our future work.

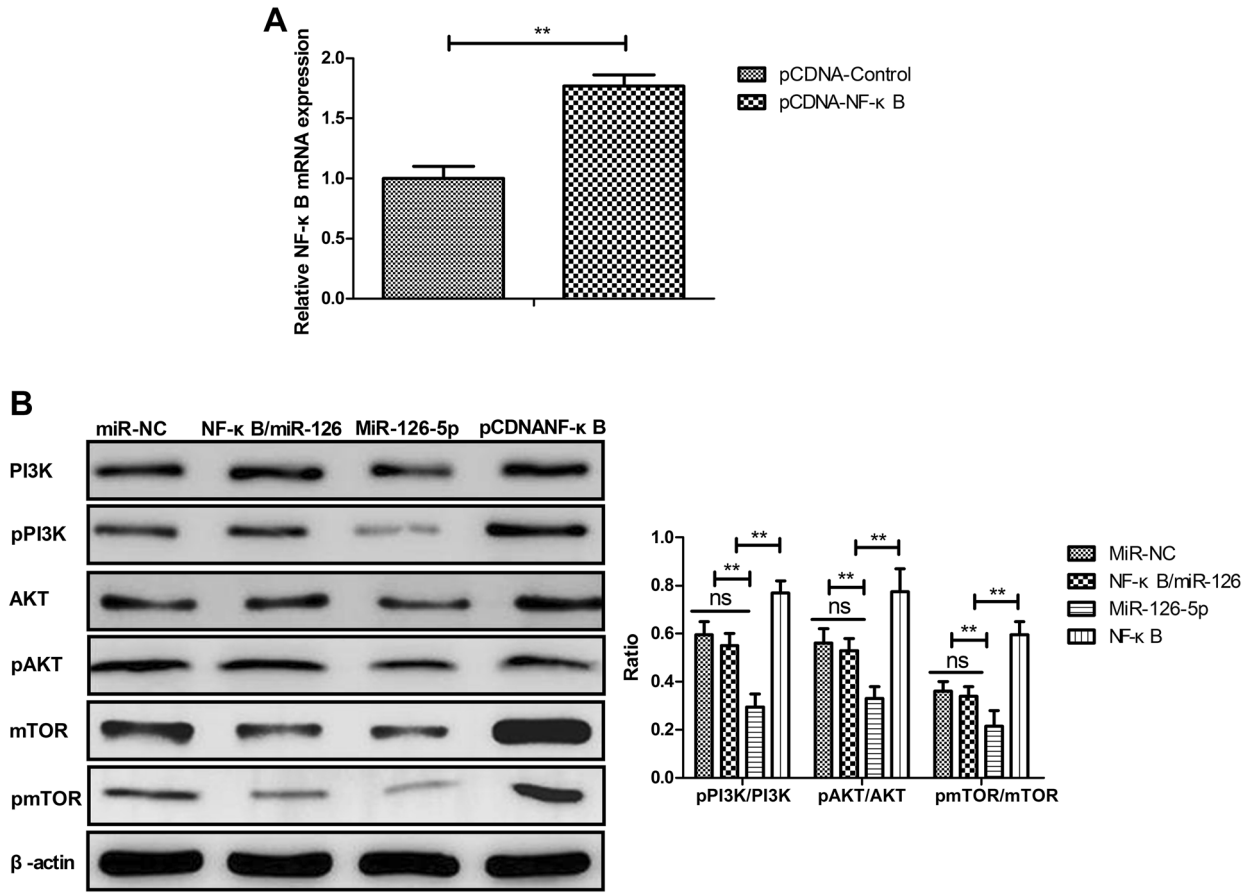

Fig. 5 MiR-126-5p inactivates NF-κB-mediated PI3K/AKT/mTOR pathway in ox-LDL-treated HAECs. **A** mRNA NF-κB expression in ox-LDL-treated HAECs after transfection with pCDNA-NF-κB. **B** Effects of NF-κB overexpression on miR-126-5p-decreased PI3K/AKT/mTOR in ox-LDL-treated HAECs. **p < 0.01 vs. miR-NC group

Conclusions

Data in this study suggest that miR-126-5p suppresses apoptosis in the aorta tissue and decreases blood lipid in apoE$^{-/-}$ mice. Data in the current study indicate that miR-126-5p mediates oxidative stress-induced apoptosis of HAECs in vascular arterial walls through suppression of the NF-κB/PI3K/Akt/mTOR signaling pathway, which may be a promising therapeutic candidate for the treatment of atherosclerosis.

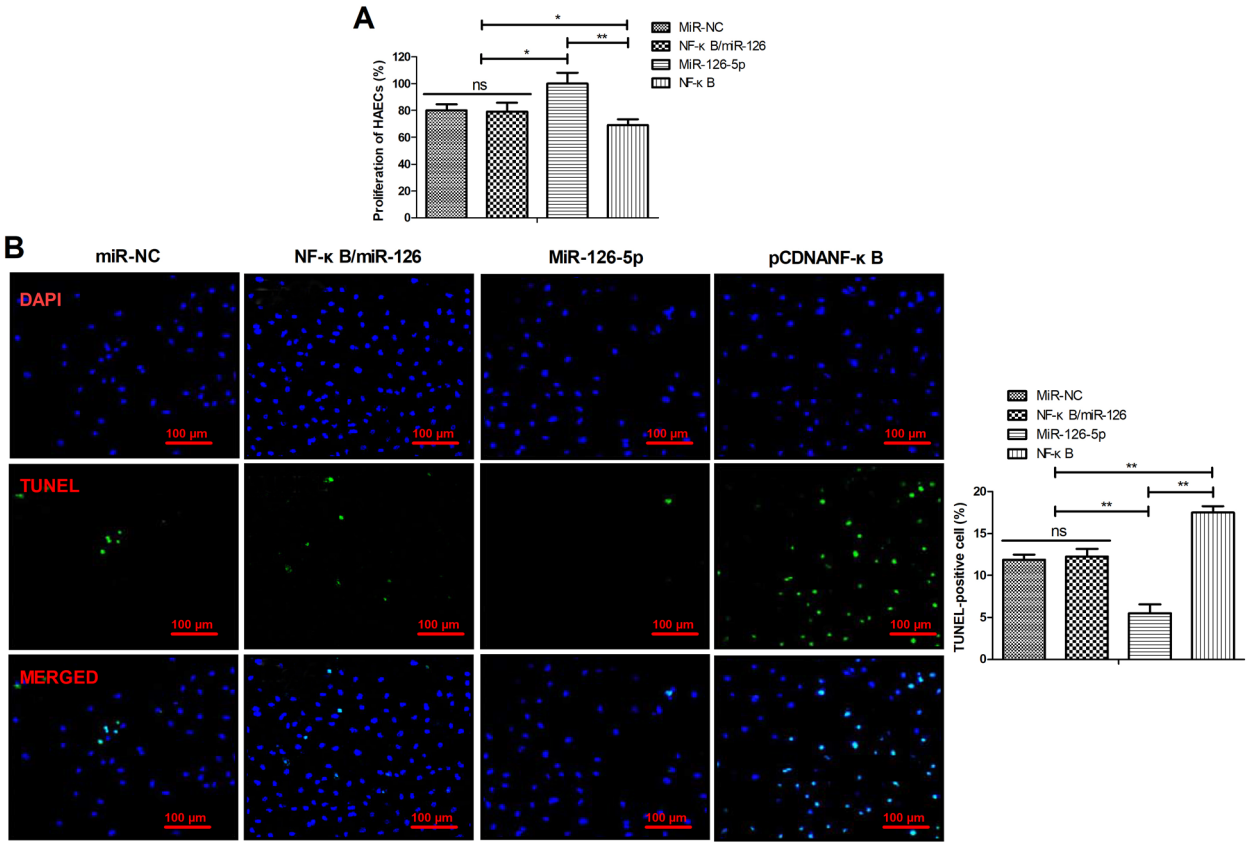

Fig. 6 Effects of NF-κB overexpression on miR-126-5p-regulated proliferation and apoptosis in ox-LDL-treated HAECs. **A**, **B** NF-κB overexpression antagonized the miR-126-5p-increased proliferation (**A**) and apoptosis (**B**) of HAECs induced by ox-LDL. **p < 0.01 vs. miR-NC group

Funding This study was supported by the Natural Science Foundation of Beijing (Grant No. 2019115BJ124).

Data availability The data used to support the findings of this study are available from the corresponding author upon request.

Declarations

Conflict of interest The author declares that he has no competing interests.

References

Altin C, Sade LE, Gezmis E, Muderrisoglu H (2016) Who is guilty of subclinical atherosclerosis in prediabetes? Chicken or egg causality paradox between insulin resistance and epicardial fat. Angiology 67:972

Boon RA, Dimmeler S (2014) MicroRNA-126 in atherosclerosis. Arterioscler Thromb Vasc Biol 34:e15-16

Bouchareychas L, Raffai RL (2018) Apolipoprotein E and atherosclerosis: from lipoprotein metabolism to MicroRNA control of inflammation. J Cardiovasc Dev Dis. https://doi.org/10.3390/jcdd5020030

Busch M, Zernecke A (2012) microRNAs in the regulation of dendritic cell functions in inflammation and atherosclerosis. J Mol Med (berl) 90:877–885

Chen WJ, Yin K, Zhao GJ, Fu YC, Tang CK (2012) The magic and mystery of microRNA-27 in atherosclerosis. Atherosclerosis 222:314–323

Chen L, Wang J, Wang B et al (2016) MiR-126 inhibits vascular endothelial cell apoptosis through targeting PI3K/Akt signaling. Ann Hematol 95:365–374

Choy JC, Granville DJ, Hunt DW, McManus BM (2001) Endothelial cell apoptosis: biochemical characteristics and potential implications for atherosclerosis. J Mol Cell Cardiol 33:1673–1690

Chu P, Han G, Ahsan A et al (2017) Phosphocreatine protects endothelial cells from Methylglyoxal induced oxidative stress and apoptosis via the regulation of PI3K/Akt/eNOS and NF-kappaB pathway. Vascul Pharmacol 91:26–35

Deng HF, Wang XL, Sun H, Xiao XZ (2017) Puerarin inhibits expression of tissue factor induced by oxidative low-density lipoprotein through activating the PI3K/Akt/eNOS pathway and inhibiting activation of ERK1/2 and NF-kappaB. Life Sci 191:115–121

Dussault S, Dhahri W, Desjarlais M, Mathieu R, Rivard A (2014) Elsibucol inhibits atherosclerosis following arterial injury: multifunctional effects on cholesterol levels, oxidative stress and inflammation. Atherosclerosis 237:194–199

Erbel C, Achenbach J, Akhavanpoor M et al (2011) PARP inhibition in atherosclerosis and its effects on dendritic cells, T cells and auto-antibody levels. Eur J Med Res 16:367–374

Gao W, Liu H, Yuan J et al (2016) Exosomes derived from mature dendritic cells increase endothelial inflammation and atherosclerosis via membrane TNF-alpha mediated NF-kappaB pathway. J Cell Mol Med 20:2318–2327

Hermann S, Kuhlmann MT, Starsichova A et al (2016) Imaging reveals the connection between spontaneous coronary plaque ruptures, atherothrombosis, and myocardial infarctions in HypoE/SRBI-/- mice. J Nucl Med 57:1420–1427

Homan R, Hanselman JC, Bak-Mueller S et al (2010) Atherosclerosis in *Octodon degus* (degu) as a model for human disease. Atherosclerosis 212:48–54

Kattoor AJ, Pothineni NVK, Palagiri D, Mehta JL (2017) Oxidative stress in atherosclerosis. Curr Atheroscler Rep 19:42

Lenato GM, Suppressa P, Giordano P et al (2007) Hereditary haemorrhagic telangiectasia: a rare disease as a model for the study of human atherosclerosis. Curr Pharm Des 13:3656–3664

Li WM, Yue JN, Guo DQ, Fu WG (2019) MiR-126 promotes endothelial cell apoptosis by targeting PI3K/Akt in rats with lower limb arteriosclerosis obliterans. Eur Rev Med Pharmacol Sci 23:327–333

Lyu QL, Jiang BM, Zhou B et al (2018) MicroRNA profiling of transgenic mice with myocardial overexpression of nucleolin. Chin Med J 131:339–346

Mao Z, Fan L, Yu Q et al (2018) Abnormality of klotho signaling is involved in polycystic ovary syndrome. Reprod Sci 25:372–383

Matulevicius S, Rohatgi A, Khera A et al (2008) The association between plasma caspase-3, atherosclerosis, and vascular function in the dallas heart study. Apoptosis 13:1281–1289

Paone S, Baxter AA, Hulett MD, Poon IKH (2019) Endothelial cell apoptosis and the role of endothelial cell-derived extracellular vesicles in the progression of atherosclerosis. Cell Mol Life Sci: CMLS 76:1093–1106

Pawlak K, Naumnik B, Brzosko S, Pawlak D, Mysliwiec M (2004) Oxidative stress - a link between endothelial injury, coagulation activation, and atherosclerosis in haemodialysis patients. Am J Nephrol 24:154–161

Rotllan N, Ramirez CM, Aryal B, Esau CC, Fernandez-Hernando C (2013) Therapeutic silencing of microRNA-33 inhibits the progression of atherosclerosis in Ldlr-/- mice–brief report. Arterioscler Thromb Vasc Biol 33:1973–1977

Santovito D, Mezzetti A, Cipollone F (2012) MicroRNAs and atherosclerosis: new actors for an old movie. Nutr Metab Cardiovasc Dis 22:937–943

Schober A, Thum T, Zernecke A (2012) MicroRNAs in vascular biology–metabolism and atherosclerosis. Thromb Haemost 107:603–604

She ZG, Zheng W, Wei YS et al (2009) Human paraoxonase gene cluster transgenic overexpression represses atherogenesis and promotes atherosclerotic plaque stability in ApoE-null mice. Circ Res 104:1160–1168

Sookoian S, Gianotti TF, Rosselli MS, Burgueno AL, Castano GO, Pirola CJ (2011) Liver transcriptional profile of atherosclerosis-related genes in human nonalcoholic fatty liver disease. Atherosclerosis 218:378–385

Tabibiazar R, Wagner RA, Ashley EA et al (2005) Signature patterns of gene expression in mouse atherosclerosis and their correlation to human coronary disease. Physiol Genom 22:213–226

Tang F, Yang TL (2018) MicroRNA-126 alleviates endothelial cells injury in atherosclerosis by restoring autophagic flux via inhibiting of PI3K/Akt/mTOR pathway. Biochem Biophys Res Commun 495:1482–1489

Viiri LE, Full LE, Navin TJ et al (2013) Smooth muscle cells in human atherosclerosis: proteomic profiling reveals differences in expression of annexin A1 and mitochondrial proteins in carotid disease. J Mol Cell Cardiol 54:65–72

von zur Muhlen C, Schiffer E, Sackmann C et al (2012) Urine proteome analysis reflects atherosclerotic disease in an ApoE-/- mouse model and allows the discovery of new candidate biomarkers in mouse and human atherosclerosis. Mol Cell Proteom. https://doi.org/10.1074/mcp.M111.013847

Wang F, Liu Z, Park SH et al (2018) Myeloid beta-catenin deficiency exacerbates atherosclerosis in low-density lipoprotein receptor-deficient mice. Arterioscler Thromb Vasc Biol 38:1468–1478

Wei Y, Nazari-Jahantigh M, Neth P, Weber C, Schober A (2013) MicroRNA-126, -145, and -155: a therapeutic triad in atherosclerosis? Arterioscler Thromb Vasc Biol 33:449–454

Xu WD, Zhang YJ, Ye DQ (2012) Evidence for a role of microRNA-146a in the pathogenesis of systemic lupus erythematosus with atherosclerosis: comment on the article by Li et al. Arthr Rheum 64:323–324

Yamawaki H, Iwai N (2006) Mechanisms underlying nano-sized air-pollution-mediated progression of atherosclerosis: carbon black causes cytotoxic injury/inflammation and inhibits cell growth in vascular endothelial cells. Circ J 70:129–140

Yao X, Yan C, Zhang L, Li Y, Wan Q (2018) LncRNA ENST00113 promotes proliferation, survival, and migration by activating PI3K/Akt/mTOR signaling pathway in atherosclerosis. Medicine 97:e0473

Yu XH, Zheng XL, Tang CK (2015) Nuclear factor-kappaB activation as a pathological mechanism of lipid metabolism and atherosclerosis. Adv Clin Chem 70:1–30

Zhang C (2009) MicroRNA and vascular smooth muscle cell phenotype: new therapy for atherosclerosis? Genome Med 1:85

Zhang T, Tian F, Wang J, Jing J, Zhou SS, Chen YD (2015a) Atherosclerosis-associated endothelial cell apoptosis by MiR-429-mediated down regulation of Bcl-2. Cell Physiol Biochem 37:1421–1430

Zhang Y, Qin W, Zhang L et al (2015b) MicroRNA-26a prevents endothelial cell apoptosis by directly targeting TRPC6 in the setting of atherosclerosis. Sci Rep 5:9401